C.P. No. 327
(18,772)
A.R C Technical Report

C.P. No. 327
(18,772)
A.R C Technical Report

MINISTRY OF SUPPLY

AERONAUTICAL RESEARCH COUNCIL

CURRENT PAPERS

The Influence of Pressure Ratio and Divergence Angle on the Shock Position in Two Dimensional, Over-Expanded, Convergent-Divergent Nozzles

By

P. F. Ashwood, and G. W. Crosse

LONDON HER MAJESTY'S STATIONERY OFFICE

1957

FOUR SHILLINGS NET

C.P. No. 327

Memorandum No. M.282

August, 1956

NATIONAL GAS TURBINE ESTABLISHMENT

The influence of pressure ratio and divergence angle on the shock position in two dimensional, over-expanded, convergent-divergent nozzles

- by -

P. F. Ashwood and G. W. Crosse

SUMMARY

Tests have been made to determine the influence of divergence angle and applied pressure ratio on the shock position in over-expanded, Laval-type, convergent-divergent nozzles. The tests covered a range of design pressure ratios between 3.5 and 17.0 and included divergence angles of from 5° to 40°.

An empirical expression has been derived which enables the limiting pressure ratio at which the nozzle just runs full to be calculated and curves are presented from which the shock position within the nozzle can be obtained.

The variation with design pressure ratio of the maximum pressure ratio obtainable across the exit shock has been determined and the results compared with those predicted using a semi-empirical formula derived from shock wave-boundary layer interaction experiments. Good agreement has been obtained.

In the absence of a suitable drying plant humid air had to be used for all the tests. The effects of this on the measured pressure distributions are discussed.

CONTENTS

APPENDICES

ILLUSTRATIONS

ILLUSTRATIONS (cont'd)

Fig. No.	Title
7	Limiting pressure ratio across exit shock
8	Variation of shock position with pressure ratio
9	Pressure recovery ratios Group 2 nozzles
10	Comparison of pressure rise parameters

C.P. No. 327

ADDENDUM

On p. 5 reference is made to the separation pressures measured by Eisenklam and Wilkie (Reference 4+) using axisymmetric conical nozzles. These authors have since pointed out that the variations in separation pressure quoted in Table 19 of Reference 4 are not significant and that for practical purposes the recovery ratio has a constant value of 2.7.

+This will be available as an Aeronautical Research Council Current Paper.

1.0 Introduction

In flight at high altitudes and high forward speeds, the use of a convergent-divergent propelling nozzle on turbo-jet or ram jet engines is essential in order to achieve the greatest possible net thrust. However, at off-design conditions, such as would occur at take-off or when flying at reduced speed, a fixed geometry divergent nozzle is inefficient due to the large negative pressure thrust which arises as the result of over expansion within the nozzle.

This can be avoided by using a variable geometry nozzle, although for some applications the complexity and weight this involves may not be warranted. Before the part-load performance of an engine fitted with a fixed divergent nozzle can be calculated, it is necessary to know under what conditions the nozzle runs full and how the position of the internal shock varies with the applied pressure ratio.

The present investigation was undertaken as part of a general programme to obtain basic data on nozzle performance.

2.0 Review of related work

Tests to investigate the phenomenon of jet separation in over-expanded supersonic nozzles have been made by a number of workers, the most important published information being contained in References 1 to 5. All of the reported tests were made at pressure ratios well below the design values so that conditions were such that flow detachment occurred well within the nozzle. In most cases it is impossible to extrapolate with any certainty to determine the limiting condition for shock at exit, a condition which is of prime importance when stimating the performance of an air breathing engine fitted with a divergent nozzle. In addition the test nozzles had values of exit/throat area varying from 3.5 to 21, so that they were more appropriate to rocket motors than to turbo-jets or ram jets.

A few of the reported investigations were made using rocket motors to supply the gas whilst the others used either compressed air or nitrogen. Due to the practical difficulty of obtaining adequate supplies of high pressure gas, "blow down" techniques had to be used with consequent limitations on running time. The rocket tests were similarly limited, the average duration of each run being about 30 seconds.

With one exception, that described in Reference 5, the conclusions drawn from all the investigations are in general agreement.

Foster and Cowles[2], using a nitric acid-aniline rocket motor fitted with various axi-symmetric conical nozzles having included divergence angles between 20° and 60°, found that for each nozzle the static pressure at the point where flow separation from the nozzle commenced tended to decrease with increasing combustion chamber pressure. For example, the pressure recovery ratio* varied between 2.52 at a chamber pressure of 12 atm. and

---

* This is the ratio of the pressure against which the nozzle is discharging (ambient for all the tests described in this Memorandum) to the pressure at the point of detachment. Thus it includes the pressure rise across the shock system together with any subsequent pressure increase due to diffusion. Most workers seem to assume that the pressure downstream of the point of detachment is always equal to the exit pressure, but the present tests do not entirely support this view.

2.97 at 26 atm. A single curve embraced all the experimental points and the influence of mixture ratio (and hence of gas temperature), nozzle area ratio and divergence angle did not appear to be great.

McKenney[3] obtained a similar result using nitrogen expanding in a two-dimensional nozzle of 30° divergence angle, the pressure recovery ratio varying between 2.5 and 2.94 as the supply pressure increased from 12 to 25 atm.

Eisenklam and Wilkie[4] also obtained similar results with air using axi-symmetric conical nozzles of 20, 30 and 40° divergence angle. For supply pressures between 14 and 34 atm. the recovery ratio varied between 2.47 and 3.02 but whilst in general the recovery ratio tended to increase with increasing supply pressure, the change was not a systematic one.

In contradiction to the results of other workers, Scheller and Bierlein[5] found that the separation pressure varied widely with both divergence angle and chamber pressure. Their tests were made with dry air on axi-symmetric nozzles having divergence angles between 10° and 66°.

Green[6] has attempted to correlate the results of a number of investigations and has suggested the use of a parameter $(P_a - P_{ks})/P_{1t}$ where P_a, P_{ks} and P_{1t} are ambient, separation and supply pressures respectively. Good correlation was obtained particularly at the higher pressure ratios, using test data obtained on nozzles of 30° divergence angle and with values of the specific heat ratio, γ, ranging between 1.23 and 1.40 and with supply pressures between 10 and 100 atm. To a large extent this agreement is inherent in the choice of the correlating parameter which is relatively insensitive to changes in the pressure recovery ratio P_{ks}/P_a, particularly at high values of P_{1t}/P_a. Although no theoretical justification was advanced for the use of the chosen parameter it is nevertheless a convenient one since it appears in the pressure thrust term of the expression for non-dimensional thrust.

3.0 Test apparatus

3.1 Model nozzle

The nozzle, which is illustrated in Figure 1, was of rectangular section with a throat approximately $\frac{1}{2}$ in. wide and 4 in. deep. To allow the divergence angle to be readily changed without altering either the entry contour or the throat area the nozzle was made up of two adjustable walls pivotted and clamped between flat side plates. The profile of each wall consisted of a circular arc entry section of 1 in. radius (i.e. two throat widths) and a flat portion tangential to the entry. To enable the effects of divergence angle and design pressure ratio to be separated the nozzle was shortened in successive stages.

The nozzle was bolted to a transition section some 3 ft in length which in turn was connected to an 8 in. diameter air supply main. The approach to the nozzle entry was faired off to a smooth contour with plaster-of-Paris.

Twenty static pressure tappings were provided along the length of one nozzle wall. The holes, which were located on a line midway between the side plates, were spaced at approximately $^5/_{16}$ in. intervals on the flat part of the nozzle wall, but were clustered together more closely on either side of the throat.

A single pitot tube fixed on the axis of the transition section was used to measure the inlet total pressure.

3.2 Method of setting the nozzle

The required divergence angle was obtained by setting the exit width with the aid of a telescopic gauge and the throat width with slip gauges. The individual positions of the static holes relative to the nozzle exit were determined separately by means of a vernier height gauge. Since the axial positions of the static tappings relative to the nozzle throat varied with the divergence angle, the appropriate corrections were applied to the measured values.

The nominal included divergence angles chosen for test were 5°, 10°, 15°, 17°, 20°, 25° and 40°. The actual values used are given in Appendix II together with the corresponding design pressure ratios, exit Mach numbers and other relevant information.

4.0 Test technique

For each nozzle setting measurement of the individual static pressures and the inlet total pressure and temperature were made with the air supply pressure increasing gradually in stages. At the conclusion of each set of tests the nozzle was shortened and the procedure repeated. In all four different lengths, making a total of 19 different nozzle designs, were tested.

Since the maximum supply pressure did not greatly exceed 9 atm., the design condition of several of the nozzles could not be reached, although in the majority of cases the available pressure was sufficient to place the shock system downstream of the nozzle exit. In view of this limitation it was necessary to establish whether any hysteresis could be observed in the pressure ratio required to position the shock at the exit plane. For this purpose several tests were made using the 17° Group 4 nozzle but no effect could be detected.

Each nozzle was tested over a range of entry pressures of from 1 to 9 atm. absolute. This resulted in the Reynolds number varying similarly, the extreme values (based on throat velocity and throat width) being about 2.5×10^5 and 1.7×10^6. No attempt was made to investigate the effects of Reynolds number in isolation, but this was not regarded as a serious omission since experiments on shock wave-boundary layer interaction suggest that flow detachment phenomena are not significantly affected by change of Reynolds number.

5.0 Effects of air humidity

As no drying plant was available to deal with the air quantities involved, humid air had to be used for all the tests described in this Memorandum.

The air supply was taken from atmosphere into a multi-stage centrifugal compressor, through an after-cooler and thence to the test nozzle. During each test the compressor speed was adjusted so that delivery pressure was only slightly in excess of that required at the nozzle and the final control obtained by means of an inlet throttle valve. Since the temperature at inlet to the nozzle was always in the region of $20^\circ C$, it can readily be shown that under conditions where the inlet control valve was fully open the

air entering the nozzle was always completely saturated. This was true over the entire range of supply pressures covered by the tests, that is from about 3 to 9 atm. absolute. Throttling between the compressor and the nozzle causes the relative humidity to decrease, but it is unlikely that this effect was very great in the majority of the tests.

The effects of humidity on the flow in supersonic nozzles have been examined theoretically and experimentally by Oswatitsch[7]. A more general discussion of the phenomena, and an analysis of tests results is contained in Reference 8.

It is shown in Reference 8 that for small nozzles a condensation shock will occur at a point where the adiabatic supercooling has reached about 55°C. Thus, for saturated air with an initial stagnation temperature of 20°C, the Mach number before the condensation shock will be 1.075. It is further shown in Reference 8 that one dimensional theory can be used to predict the changes of state that occur across the condensation shock if the amount of water vapour condensed is chosen (by trial and error calculation) so that the remaining water vapour is saturated after the shock. This assumption has been found to correspond, at least in the tests analysed in Reference 8, to the condition for the maximum heat addition theoretically possible. This condition results in the Mach number after the shock being equal to unity. The absolute humidity after the shock is so small that no further condensation effects of appreciable magnitude occur.

Sample calculations illustrating the changes of state due to a condensation shock are given in Appendix III.

6.0 Analysis of results

For each nozzle arrangement a graph was prepared showing the axial variation of the static pressure for the various applied pressure ratios. The method adopted for plotting the results was the one used by Binnie and Woods[9] in which P_{xs}/P_{it} is plotted against x/d. Two typical graphs are shown in Figures 2 and 3.

Since the number of static points was limited, it was often difficult, with the method of plotting used in Figures 2 and 3, to decide on the exact shape of the pressure distribution curve immediately downstream of the shock. The shock position could not therefore be precisely determined. To overcome this difficulty the results were cross-plotted to determine at what overall pressure ratios the shock occurred* exactly at the position of the various static tappings. Such a curve is shown in Figure 4 which is a re-plot of the results given in Figure 2. Since for any given point the ratio P_{xs}/P_{it} remains constant once the shock has moved downstream of the point considered, the curves of Figure 4 show well defined discontinuities. The overall pressure ratios corresponding to the shock being located at each of the static tappings is thus easily determined.

The kink points obtained from Figure 4 were then plotted in the form shown in Figure 5 to give the variation of shock position with applied

---

* One dimensional analysis of the flow enables the shock position to be specified right to the flow boundary. In practice, however, viscous effects modify the shock structure with the result that at the boundary the influence of the shock extends further upstream than the elementary theory suggests. The term 'shock position' as used in this Memorandum refers strictly to the furthermost upstream position at which the influence of the shock can be detected at the walls.

pressure ratio. The shock position is expressed in terms of the throat width, d. Extrapolation of each curve to that value of x/d representing the exit plane enabled the limiting pressure ratios for shock at exit, $(P_{1t}/Pa)_{lim}$, to be determined.

Examination of the pressure distribution curves for complete expansion given in Figures 2 and 3, which are typical of all the nozzles tested, shows that in the case of the 10° Group 2 nozzle (Figure 2) the measured pressures commence to depart from the one-dimensional isentropic values just upstream of the throat, whereas for the 5° Group 3 nozzle (Figure 3) the expansion follows the isentropic curve for some distance downstream of the throat then exhibits a sudden upward jump. The reason for the first effect is obscure but the latter is almost certainly due to the presence of a condensation shock. Specimen calculations illustrating the magnitude of the pressure rise due to a condensation shock are given in Appendix III and it is shown that the pressure rise depends on the humidity of the air entering the nozzle and on the stagnation temperature. Although no measurements were made of the humidity of the air supply, it has already been pointed out (Section 5.0) that for the majority of the tests the relative humidity at entry to the nozzle must have been close to unity. Thus with an adiabatic supercooling of 55°C, the Mach number before the condensation shock would be at least 1.07 at which point the value of P_{xs}/P_{1t} would be 0.404. The results shown in Figure 3 suggest that for this test at least the condensation shock occurred at a value of P_{xs}/P_{1t} in the region of 0.4, that is at a Mach number of 1.22. To obtain this value by the method of Appendix III it is necessary to assume either that the air entering the nozzle was not completely saturated or that the adiabatic supercooling exceeded 55°C. In view of the close agreement between the results of different workers concerning the amount of supercooling obtainable, the first of these alternatives appears to provide the only possible explanation.

Even if the higher pre-shock Mach number is assumed, however, the measured pressure distribution with the nozzle running full cannot be exactly accounted for by the method suggested in Reference 8, which assumes that all the heat is added instantaneously and that the flow on either side of the condensation shock is one-dimensional and isentropic. In the following Section it is noted that the greater part of the difference can be explained as being due to skin friction.

The flow changes which occur when the pressure supplied to a nozzle discharging to atmosphere is progressively reduced from the design value are well known. Expansion proceeds to a pressure below the ambient and a shock system is set up at the nozzle outlet to restore the exit pressure to that of the surrounding atmosphere. Ultimately a point is reached when the boundary layer is unable to support the required pressure gradient and the flow then detaches from the walls of the nozzle and the shock system moves upstream. One-dimensional theory assumed that this will not happen until the applied pressure ratio is such that a normal shock is required at exit to restore the pressure to ambient, but in practice this condition is never achieved and detachment of the flow occurs at substantially higher pressure ratios than predicted by the simple theory.

6.1 Nozzle over-expanded, shock downstream of exit plane

The results of all the present tests are shown in Figure 6 in which the nozzle pressure ratio, P_{1t}/P_{1s}, and the minimum applied pressure ratio

for the shock to remain at exit, $(P_{1}t/P_{a})_{lim}$, are plotted against the design pressure ratio, E. Divergence angle appears to have only a second order effect and over the range covered by the tests (i.e. $3.5<E<17$) all the experimental points lie close to the two straight lines defined by the equations:-

$$P_{1}t/P_{3}s = 0.92E \quad .. \quad .. \quad .. \quad .. \quad (1)$$

and

$$(P_{1}t/P_{a})_{lim} = 1 + 0.39E \quad .. \quad .. \quad .. \quad .. \quad (2)$$

The fact that the constant of proportionality in Equation (1) does not equal unity indicates the extent to which the expansion departs from the isentropic. Calculations show that the major reason for the discrepancy is the loss due to skin friction and the assumption of a friction factor $a = \gamma f/2\tan\beta = 0.05$ enables almost all the difference to be accounted for. The presence of a condensation shock accounts for a small proportion of the pressure loss, (about one-eighth).

Equations (1) and (2) can be combined to give the maximum pressure ratio obtainable across the exit shock before it commences to move inside the nozzle. Thus,

$$\text{Pressure ratio across exit shock} = P_{a}/P_{3}s$$

$$= P_{a}/P_{1}t \times P_{1}t/P_{3}s$$

Hence from Equations (1) and (2)

$$(P_{a}/P_{3}s)_{lim} = \frac{0.92E}{1 + 0.39E} \quad .. \quad .. \quad .. \quad (3)$$

The right-hand side of this expression becomes equal to unity when $E = 1.89$, the critical pressure ratio for air. Its magnitude for other values of E is given in Table I below.

TABLE I

Maximum pressure rise obtainable across exit shock

E	$P_{1}t/P_{3}s$	$(P_{1}t/P_{a})_{lim}$	$\left(\frac{P_{a}}{P_{3}s}\right)_{lim}$
20	18.4	8.8	2.09
15	13.8	6.85	2.02
10	9.2	4.9	1.88
5	4.6	2.95	1.56
4	3.68	2.56	1.44

Figure 7 gives a comparison between the values obtained from Equation (3) and those calculated from a semi-empirical expression derived from shock wave-boundary layer interaction experiments and quoted in Reference 10. Agreement between the two sets of results is quite good, particularly in view of the fact that the tests of Reference 10 were made with uniform, parallel flow, a condition which does not apply to the nozzle tests.

6.2 Nozzle over-expanded, shock within the nozzle

Graphs of the type shown in Figure 5 enable the variation of the shock position with overall pressure ratio to be determined and this was done for several of the nozzle configurations tested. It was found that for values of E greater than about 8 the relative pressure ratio, Δ, (Δ = applied pressure ratio/design pressure ratio) required to place the shock at any given value of A_{shock}/A_{exit} was completely independent of the divergence angle and virtually independent of the design pressure ratio.

Numerical values obtained from the test results enabled the variation of the shock position to be determined. This was done for four nozzles and the results of these calculations are shown in Figure 8.

For conditions where the shock lies within the nozzle it is impossible from the results of the present tests to determine just how much of the pressure recovery occurs across the shock and how much is due to diffusion of the flow after the shock system.

Figure 9 shows the variation of pressure recovery ratio, P_a/P_{ks}, with the pressure ratio up to the shock position, $P_{1}t/P_{ks}$, for the Group 2 nozzles. If no recovery occurred the pressure after the shock would be atmospheric. The portion of the nozzle downstream of the shock could therefore be ignored and conditions would be the same as in the case of limiting shock at exit for a nozzle of reduced length. The test points would then lie on the dotted curve which has been plotted from Equation (3). However, considerable recovery does occur, a fact indicated by the departure of the experimental points from the dotted curve. As would be expected the departure is most noticeable for the 5° divergence angle and tends to decrease with increasing angle.

In Figure 10 the results are shown in the form suggested by Green in Reference 6, that is with $(P_a - P_{ks})/P_{1}t$ plotted against $P_{1}t/P_a$. Points corresponding both to conditions of shock within the nozzle and at exit are included on the graph. A single curve has been drawn through all the experimental points, a procedure which cannot strictly be justified since it ignores the effects of area ratio and divergence angle. However, the scatter is not excessive. The equation to the curve best fitting the points is:

$$\frac{P_a - P_{ks}}{P_{1}t} = \frac{0.49}{P_{1}t/P_a} \qquad .. \quad .. \quad .. \quad (4)$$

which can be recast as:

$$P_{ks} = (1 - 0.49)P_a$$

giving

$$P_{ks}/P_a = 0.51 \qquad .. \quad .. \quad .. \quad .. \quad (5)$$

This result agrees qualitatively with a comment made by Summerfield[11] to the effect that work at the California Institute of Technology has shown that separation in nozzles discharging to atmosphere occurs at a constant static pressure of roughly 0.4 atm.

For comparison, values obtained from the curve given by Green are also included on Figure 10. To obtain these accurately for values of $P_{1}t/P_a$ below 5, it was necessary to extrapolate the published curve and this was done by determining the equation which best fitted Green's results and using this to calculate the required values.

It will be seen that at low pressure ratios the measured values of $(P_a - P_{ks})/P_{1}t$ are considerably higher than those predicted by the curve of Reference 6, but as the pressure ratio increases the difference becomes less.

Values of $(P_a - P_{ks})/P_{1}t$ for the limiting case of shock at exit can be calculated using Equations (1) and (2) and this gives the chain dotted curve shown in Figure 10. At pressure ratios in excess of 5 agreement with the mean curve drawn through the measured values is quite good, but at lower pressure ratios the curves diverge. This is due to the pressure recovery which occurs after the shock when detachment occurs well within the nozzle at a point when the Mach number is relatively low. The effect can best be explained by means of a numerical example.

Consider a nozzle having a design pressure ratio, E, of 10.23. From Equation (2) the limiting pressure ratio for the shock to remain at exit is $(1 + 0.39 \times 10.23) = 5.0$ and the limiting pressure ratio across the shock is then $0.92 \times 10.23/5 = 1.88$.

Suppose now the overall pressure ratio is reduced to 2.5. If no pressure rise occurred after the shock, that part of the nozzle downstream of the point of detachment could be discarded and the flow treated as being the shock-at-exit case for a nozzle of smaller design pressure ratio. From Equation (2) the new value of E would then be $(2.5 - 1)/0.39 = 3.84$ and the pressure ratio across the shock (from Equation (3)) $0.92 \times 3.84/2.5 = 1.41$. The pressure before the shock would be $1/1.41 = 0.705$ atm. However, Equation (5), which is based on test results, gives the pressure before the shock as 0.51 atm. so that $P_{1}t/P_{ks} = 2.5/0.51 = 4.9$. From Figure 8 the pressure ratio across the shock corresponding to this value of $P_{1}t/P_{ks}$ is 1.58 so that the pressure after the shock is $1.58 \times 0.51 = 0.805$ atm. Therefore, a further pressure rise from this value to atmospheric pressure must evidently occur between the shock and the nozzle exit.

It follows therefore, that calculations in which the pressure recovery after the shock is neglected will give an estimated shock position which is too far upstream. It is also clear that knowledge of the pressure distribution after the shock is necessary in order to calculate the thrust developed by an over-expanded nozzle in which the shock is upstream of the exit plane.

7.0 Conclusions

Tests have been made using cold air to determine the static pressure distributions and shock positions at conditions of over-expansion for a series of two-dimensional, Laval-type, convergent-divergent nozzles covering a range of design pressure ratios between 3.5 and 17 and included

divergence angles of from 5° to 40°. As no drying plant of suitable capacity was available, humid air had to be used for all the tests.

Although the use of humid air influences the static pressure distribution within the nozzle due to the formation of a condensation shock, it is thought that the measurements of the pressure recovery ratio and of the maximum pressure ratio obtainable across the exit shock are not likely to be seriously affected. This argument is supported by the good agreement obtained with the results of tests made by other workers using dried air.

It has been shown that for divergent nozzles expanding air, the lowest pressure ratio at which the shock can be maintained beyond the nozzle exit plane is insensitive to divergence angle and is given by:

Limiting pressure ratio
for shock at exit = 1 + 0.39 × design pressure ratio.

At pressure ratios below the limiting value the shock system lies within the nozzle. The present tests show that the pressure at which separation occurs is given by:

Separation pressure = 0.51 × ambient pressure.

This result is substantially independent of divergence angle and design pressure ratio.

The tests have shown that an appreciable pressure rise can occur after the shock particularly with nozzles having small divergence angles and therefore knowledge of the pressure distribution is necessary in order to calculate the thrust developed by an over-expanded nozzle.

REFERENCES

No.	Author	Title
1	Summerfield M., Foster C. R. and Swan W. C.	Flow separation in over-expanded supersonic exhaust nozzles. Jet propulsion Vol. 24 pp. 319-321, 1954.
2	Foster C. R. and Cowles F. B.	Experimental study of flow separation in over-expanded exhaust nozzles for rocket motors. J.P.L. Progress Report No. 4-103, May 1949, California Institute of Technology (TIB P.41004).
3	McKenney J. D.	An investigation of flow separation in an over-expanded supersonic nozzle. Thesis for A.C.T., California Institute of Technology, 1949, (Abstract given in Reference 1).
4	Eisenklam P. and Wilkie D.	On jet separation in supersonic rocket nozzles. Part I The characteristics of flow. Imperial College Report J.R.L. No. 29. May, 1955, (M.O.S. Reference DGCW Report/ EMR/55/4). A.R.C. 18,438. May, 1955.
5	Scheller K. and Bierlein J. A.	Some experiments on flow separation in rocket nozzles. Jour. Am. Rocket Soc. Vol. 23 pp. 28-32, 1953.
6	Green L.	Flow separation in rocket nozzles. Jour. Am. Rocket Soc. Vol. 23 pp. 34-35, 1953.
7	Oswatitsch K.	Condensation phenomena in supersonic nozzles. Z.A.M.M. Vol. 22, pp. 1-14, 1942. (Available as translation Reference R.T.P. Trans. No. 1905). A.R.C. 7057.
8	Lukasiewicz J. and Royle J. K.	Effects of air humidity in supersonic wind tunnels. R. & M. 2963, 1953.
9	Binnie A. M. and Woods M. W.	Pressure distribution in a convergent-divergent steam nozzle. Proc. I. Mech. E. Vol. 138 pp. 208-226. 1938.
10	Gadd G. E.	A semi-empirical theory for inter-actions between turbulent boundary layers and shock waves strong enough to cause separation. A.R.C. 15,543, January, 1953.
11	Summerfield M.	Fundamental problems in rocket research. Jour. Am. Rocket Soc. June, 1950.

APPENDIX I

Notation

A	Nozzle area
d	Nozzle throat width
E	Design pressure ratio (isentropic)
f	Friction coefficient
M	Mach number
P_a	Ambient pressure
P_s	Static pressure
P_t	Total pressure
x	Length along nozzle axis measured from throat
Δ	Applied pressure ratio relative to design $\left(= \frac{P_{1t}/P_a}{E}\right)$
β	Nozzle divergence half angle
γ	Specific heat ratio

Subscripts 1, 2 and 3 refer to stations at the nozzle entry, throat and exit respectively. Subscript 'x' is used to denote a generalised station distant x from the throat, and subscript 'k' the point at which the shock occurs within the nozzle.

APPENDIX II

Design details of test nozzles

Group	Axial length (inches)	Included divergence angle		Measured area ratio	Isentropic design pressure ratio	Design exit Mach number
		Nominal	Actual			
1	3.127	5°	4° 50'	1.518	6.41	1.87
	3.166	10°	9° 40'	2.054	11.17	2.23
	3.200	15°	14° 14'	2.580	16.45	2.48
2	2.481	5°	4° 38'	1.392	5.37	1.75
	2.520	10°	10° 0'	1.835	9.13	2.10
	2.556	15°	14° 2'	2.242	12.99	2.32
	2.640	17°	18° 0'	2.660	17.32	2.51
3	1.543	5°	4° 52'	1.258	4.30	1.61
	1.586	10°	9° 24'	1.514	6.36	1.87
	1.620	15°	13° 42'	1.770	8.55	2.06
	1.718	17°	17° 06'	2.023	10.90	2.21
	1.737	25°	24° 46'	2.521	15.73	2.45
4	0.905	5°	4° 46'	1.147	3.14	1.45
	0.948	10°	9° 30'	1.310	4.70	1.67
	0.985	15°	13° 14'	1.451	5.85	1.81
	1.082	17°	17° 6'	1.645	7.46	1.97
	1.096	20°	21° 20'	1.825	9.04	2.09
	1.104	25°	26° 12'	2.037	11.01	2.22
	1.187	40°	39° 0'	2.580	14.37	2.39

APPENDIX III

Effects of condensation shock

All the tests described in this Memorandum were made during the Winter months. For typical Winter conditions, ($T = 0^{\circ}C$, relative humidity = 0.8), the absolute humidity is 0.0038 lb water vapour/lb air. Saturated air at a pressure and temperature of 9 atm. and $20^{\circ}C$ contains 0.0016 lb water vapour/lb air and hence more than half the water vapour present in the air aspirated into the compressor must condense out in the aftercooler when the air is cooled to this temperature. If the air is cooled to $30^{\circ}C$, then at 9 atm. pressure it contains 0.0029 lb water vapour/lb air when saturated.

Therefore, providing no throttling occurs after the compressor, the air supplied to the nozzle must always be saturated. Calculation of the state of the air after throttling is quite straightforward since the stagnation temperature remains unaltered during the process. To determine the point at which a condensation shock occurs, it is necessary first to calculate the temperature at which saturation is reached. The temperature before condensation then follows from the assumed degree of supercooling and hence the Mach number and pressure ratio across the shock. The example given below illustrates the method:

Calculation of changes of state across condensation shock

Assumed entry conditions:

Stagnation temperature	=	$293^{\circ}K$
Relative humidity	=	0.80
Total pressure	=	106 lb/sq.in.abs.

The assumed value of relative humidity is that which would be obtained by throttling saturated air at 9 atm. to the assumed entry pressure.

From Figure 21 of Reference 8, saturation will be reached at a temperature of $289^{\circ}K$. Hence, assuming an adiabatic supercooling of $55^{\circ}C$, a condensation shock will occur at a static temperature of $(289 - 55) = 234^{\circ}K$.

Temperature ratio at condensation = $293/234$ = 1.252

$\therefore$ Mach number at condensation = 1.123

Using Equation (1) of Reference 6 and putting $Z = 1$, corresponding to the condition of maximum heat release, the static pressure ratio across the shock is given by:

$$\text{Static pressure ratio} = \frac{\gamma}{\gamma + 1}(M^2 - 1) + 1$$

which for $M = 1.123$ and with $\gamma = 1.40$ gives:

$$\text{Static pressure ratio} = 1.152$$

Thus the ratio (wall static/inlet total pressure) changes from 0.455 (i.e. the value corresponding to M = 1.123 before the shock to 0.455 x 1.152 = 0.524 after the shock.

Since the Mach number after the shock is unity, the ratio of total pressure after the shock to that before is 0.524/0 528 = 0.993. The shock thus causes a loss of total pressure of 0.7 per cent.

Equations (2) and (3) of Reference 8 show the static temperature ratio across the shock to be given by:-

$$\text{Static temperature ratio} = \left[\frac{\gamma M^2 + 1}{(\gamma+1)M}\right]^2$$

which for M = 1.123 and with γ = 1.40 gives:

$$\text{Static temperature ratio} = 1.058$$

The static temperature after the shock is therefore 234 x 1.058 = 247.6°K and since the Mach number after the shock is unity the total temperature is 1.200 x 247.6 = 297.1°K. The shock thus causes a rise of 4.1°C in total temperature. This value will now be checked by compiling a heat balance.

If the air after the shock is completely saturated, then it contains 9.5×10^{-5} lb water per lb, whereas the air entering the nozzle contains 159.3×10^{-5} lb water per lb. The heat given up by the water in condensing is therefore:

$$(159.3 - 9.5) \times 10^{-5} \times 690 = 1.032 \text{ C.H.U./lb}$$

and the temperature rise of the air is $\frac{1.032}{0.24}$ = 4.3°C which agrees with the value previously determined.

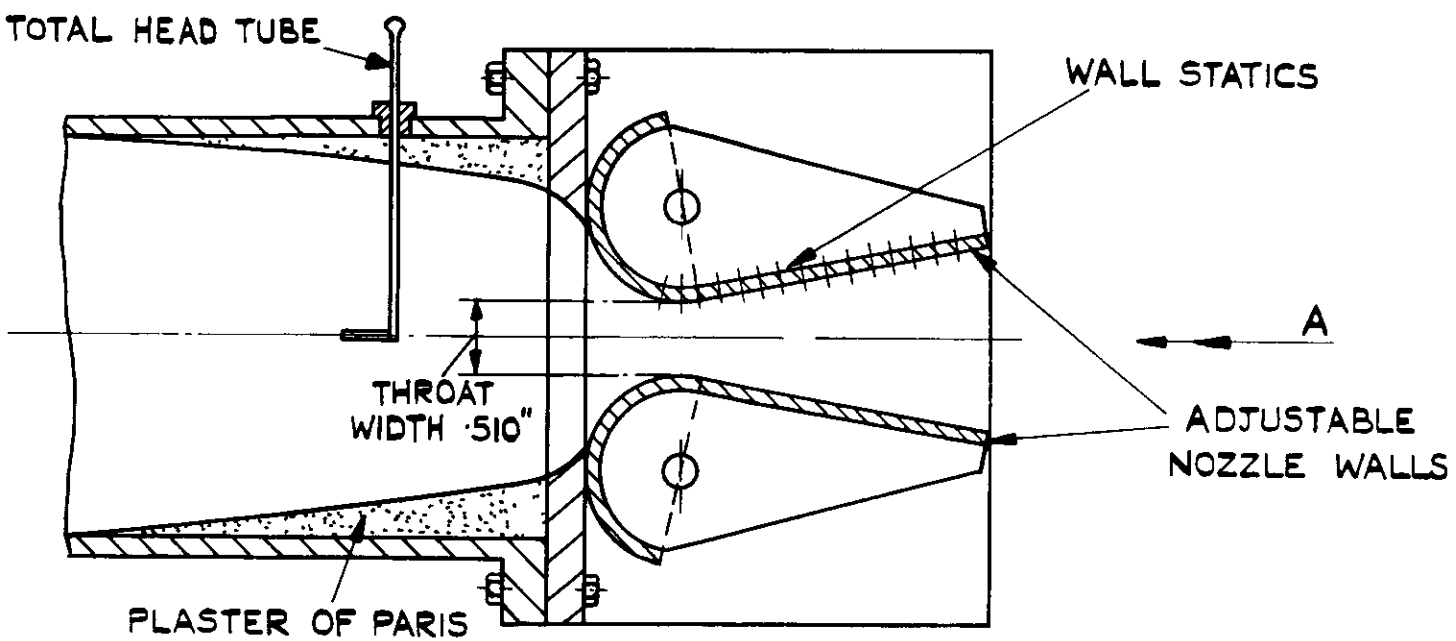

SIDE VIEW CROSS SECTION

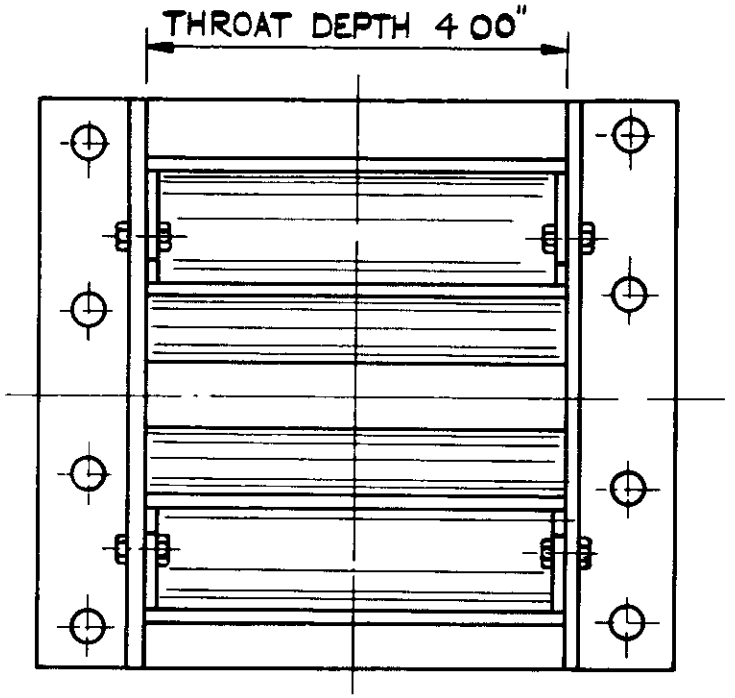

VIEW IN DIRECTION A.

TEST NOZZLE

FIG. 1

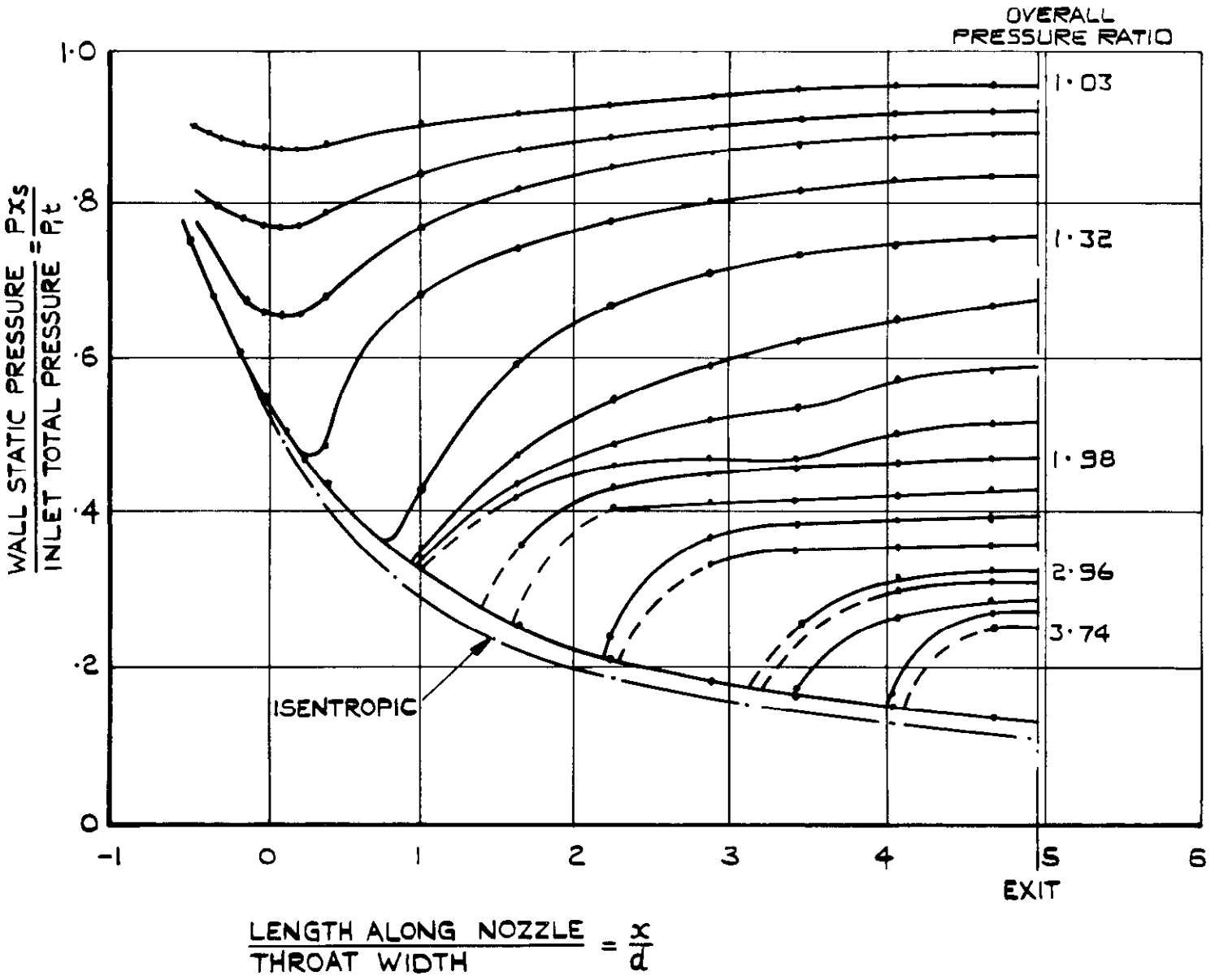

VARIATION OF STATIC PRESSURE FOR 10° GROUP 2 NOZZLE.

FIG. 2

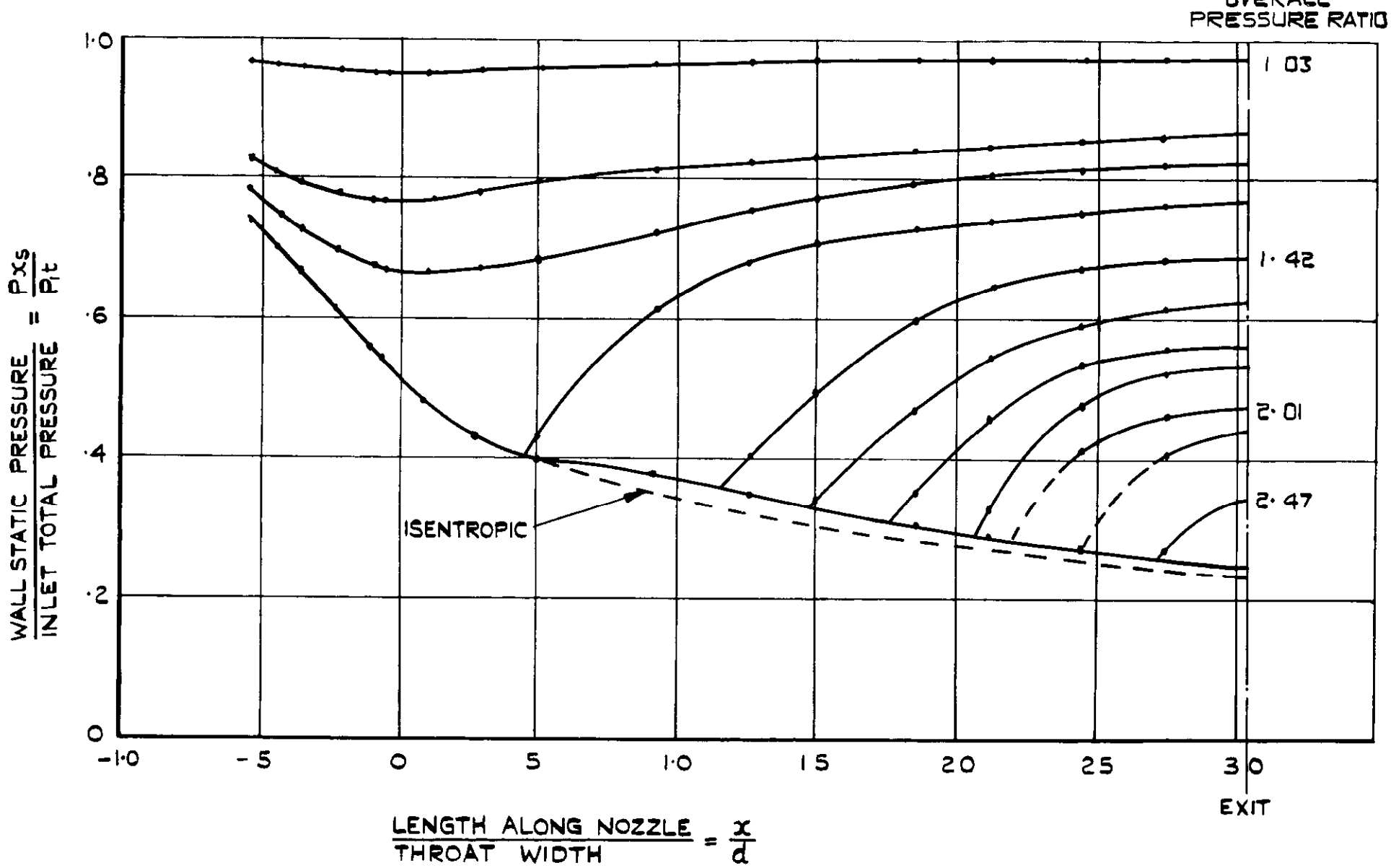

VARIATION OF STATIC PRESSURE FOR 5° GROUP 3 NOZZLE.

FIG. 3

FIG. 4

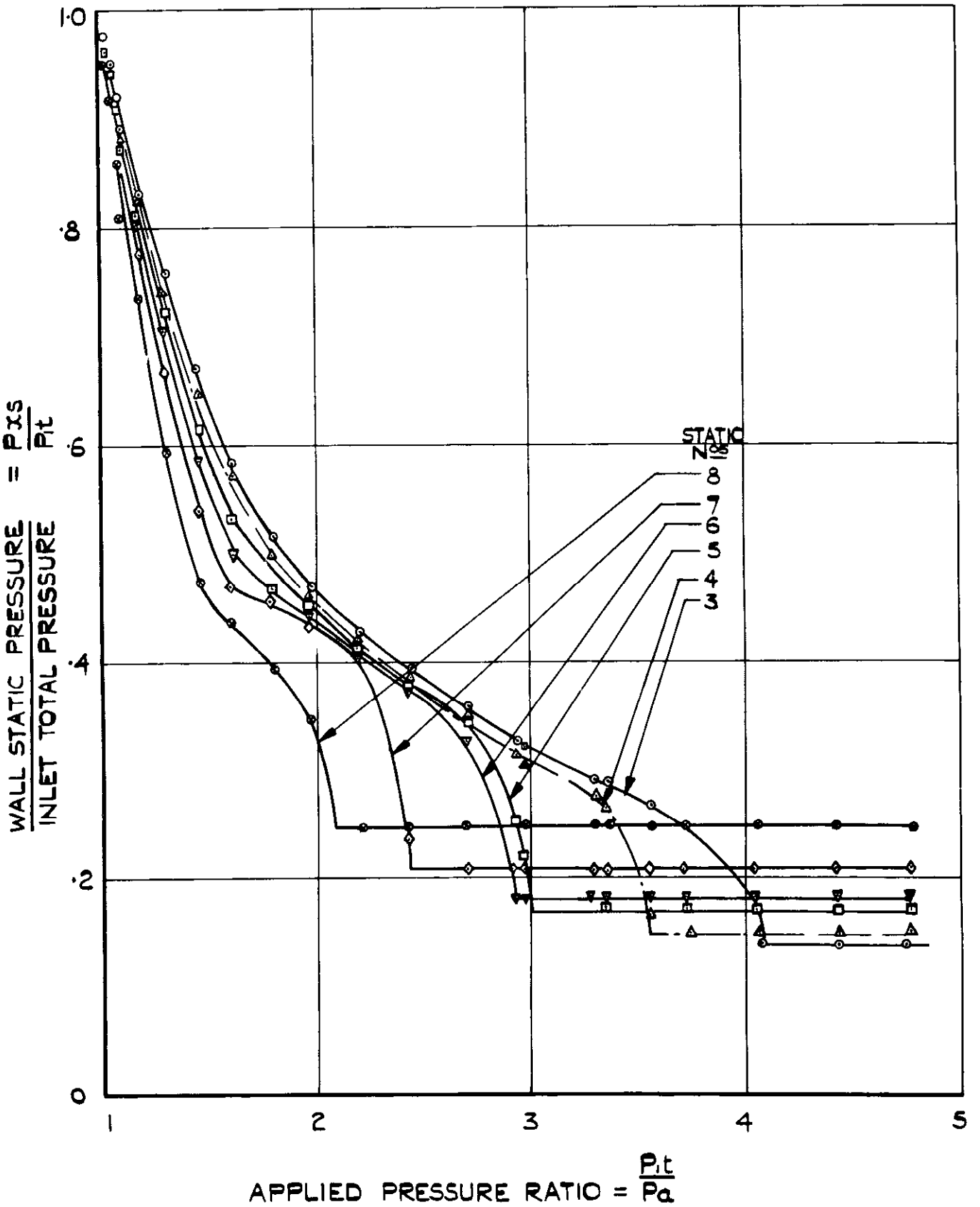

VARIATION OF WALL STATIC WITH INLET PRESSURE FOR 10° GROUP 2 NOZZLE.

FIG. 5

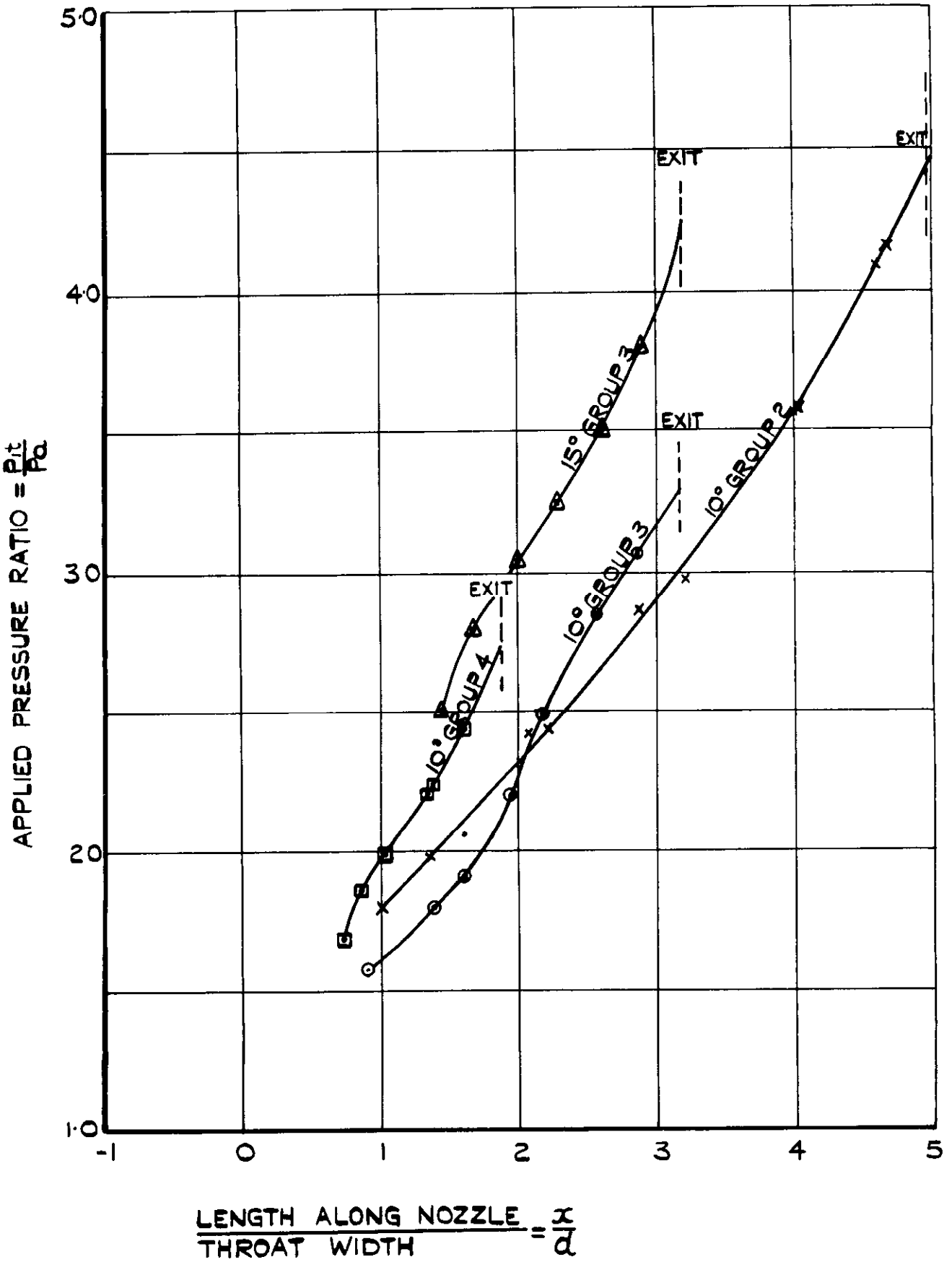

VARIATION OF SHOCK POSITION WITH PRESSURE RATIO.

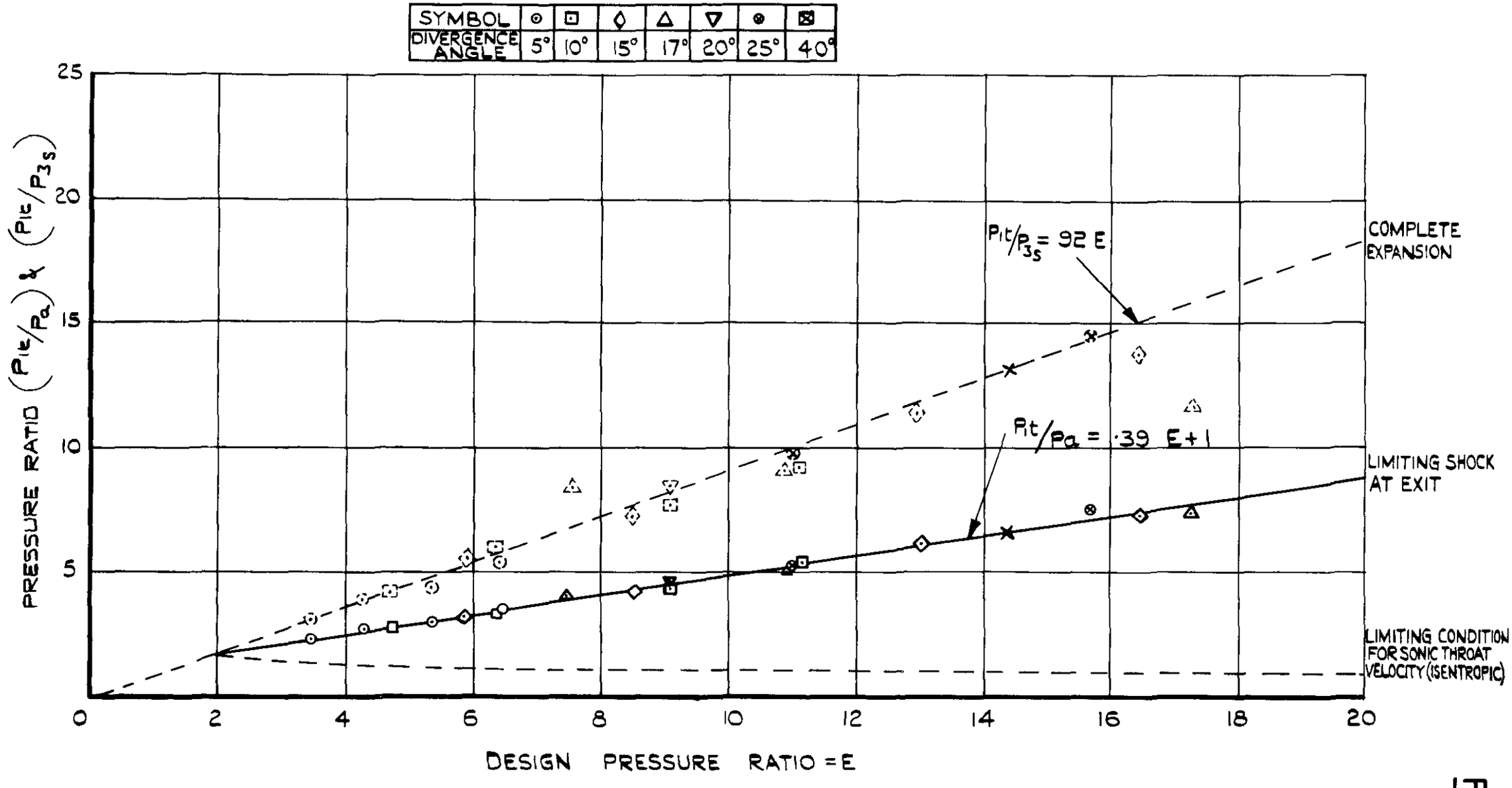

PRESSURE RATIOS FOR SHOCK AT EXIT & COMPLETE EXPANSION.

FIG. 6

FIG. 7.

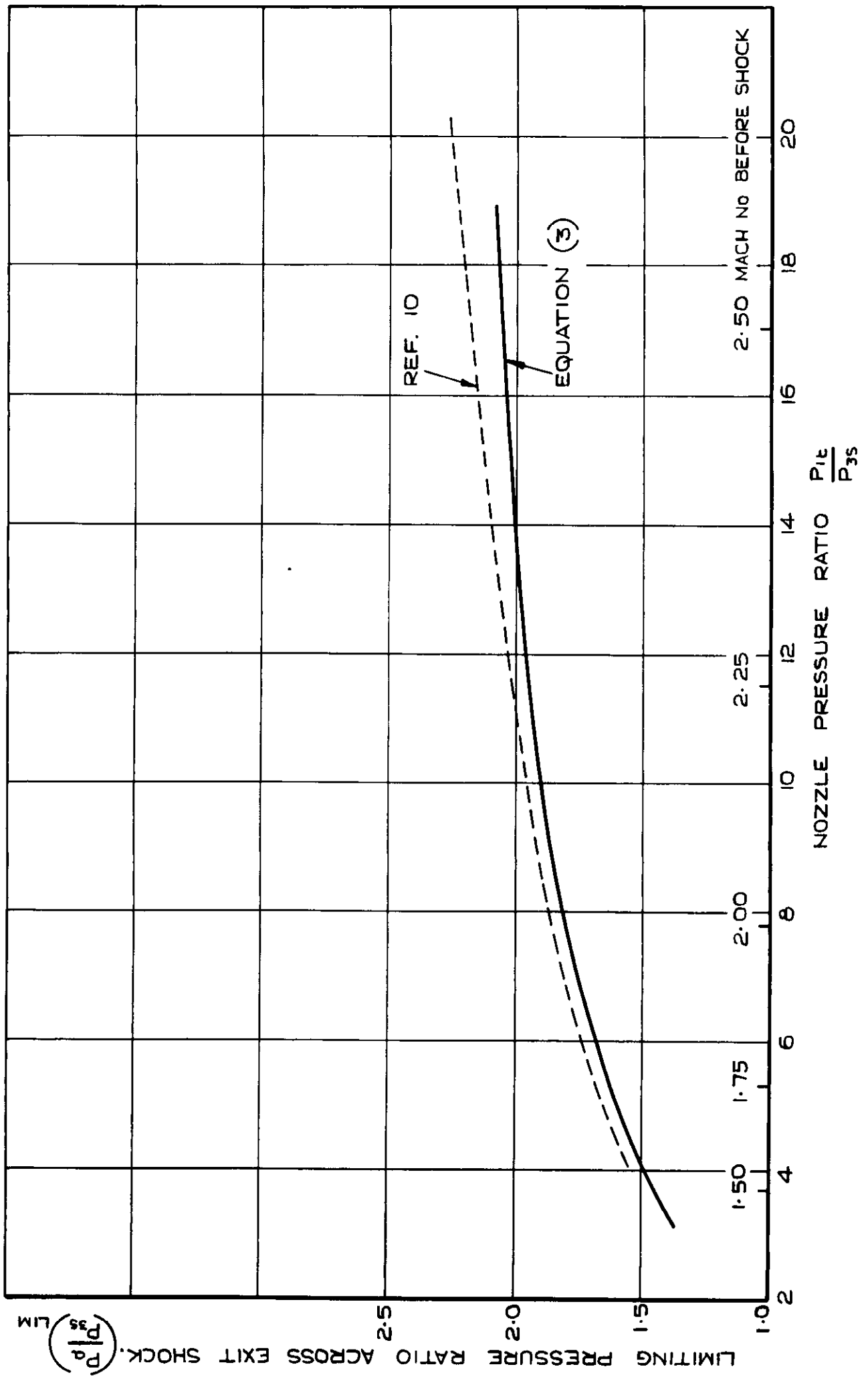

LIMITING PRESSURE RATIO ACROSS EXIT SHOCK.

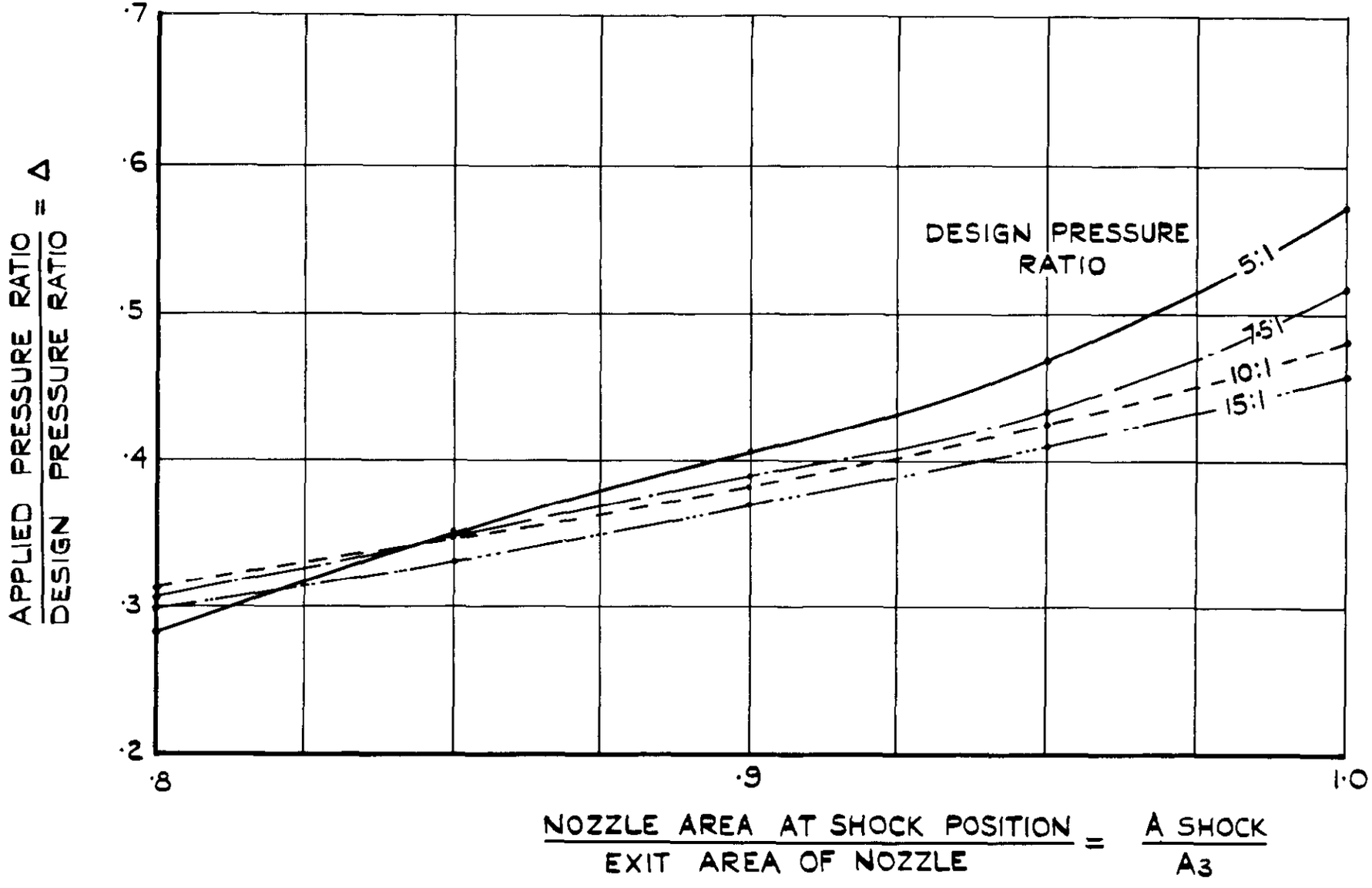

VARIATION OF SHOCK POSITION WITH PRESSURE RATIO.

FIG.8

FIG. 9

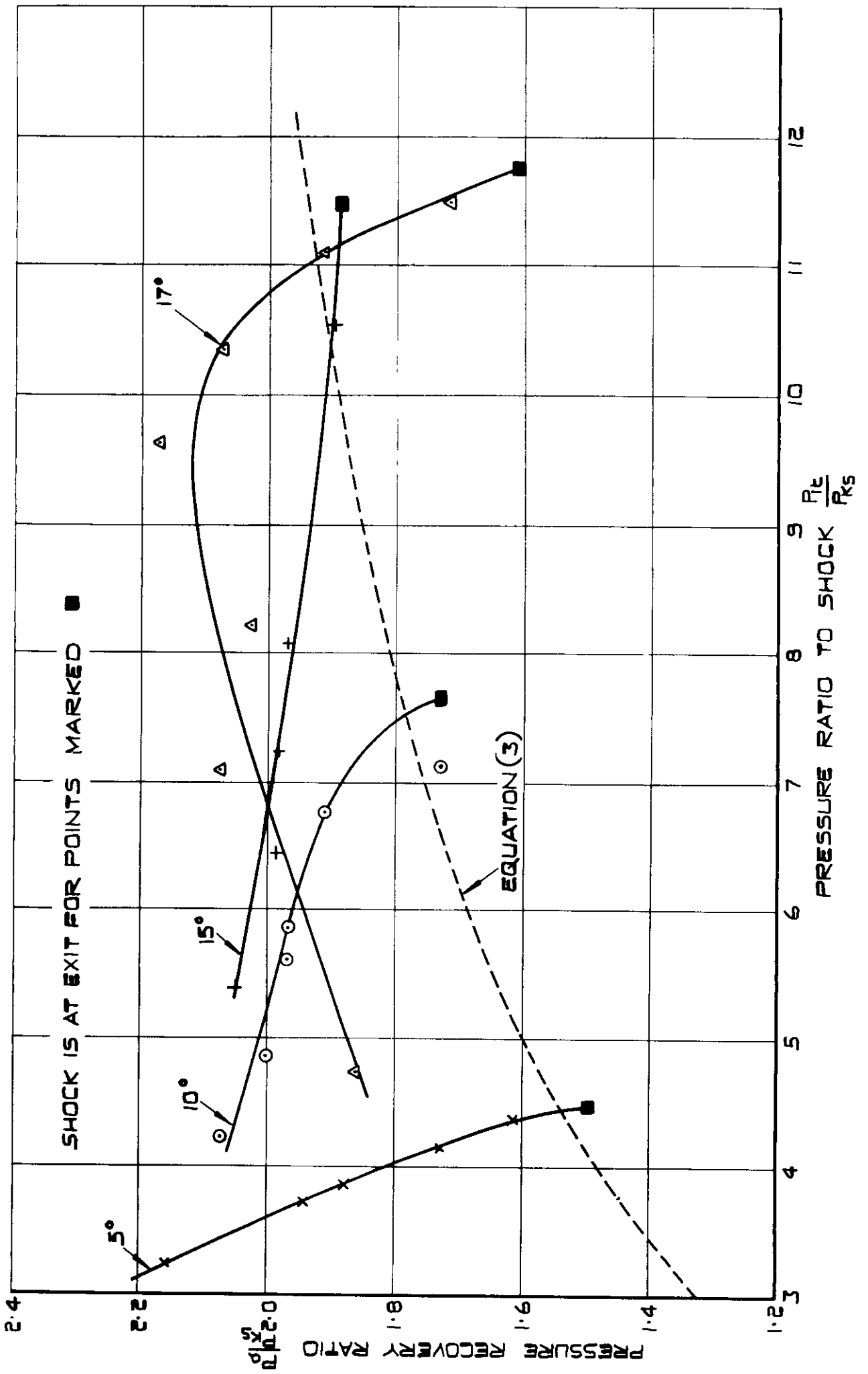

PRESSURE RECOVERY RATIOS

GROUP 2 NOZZLES.

FIG. 10.

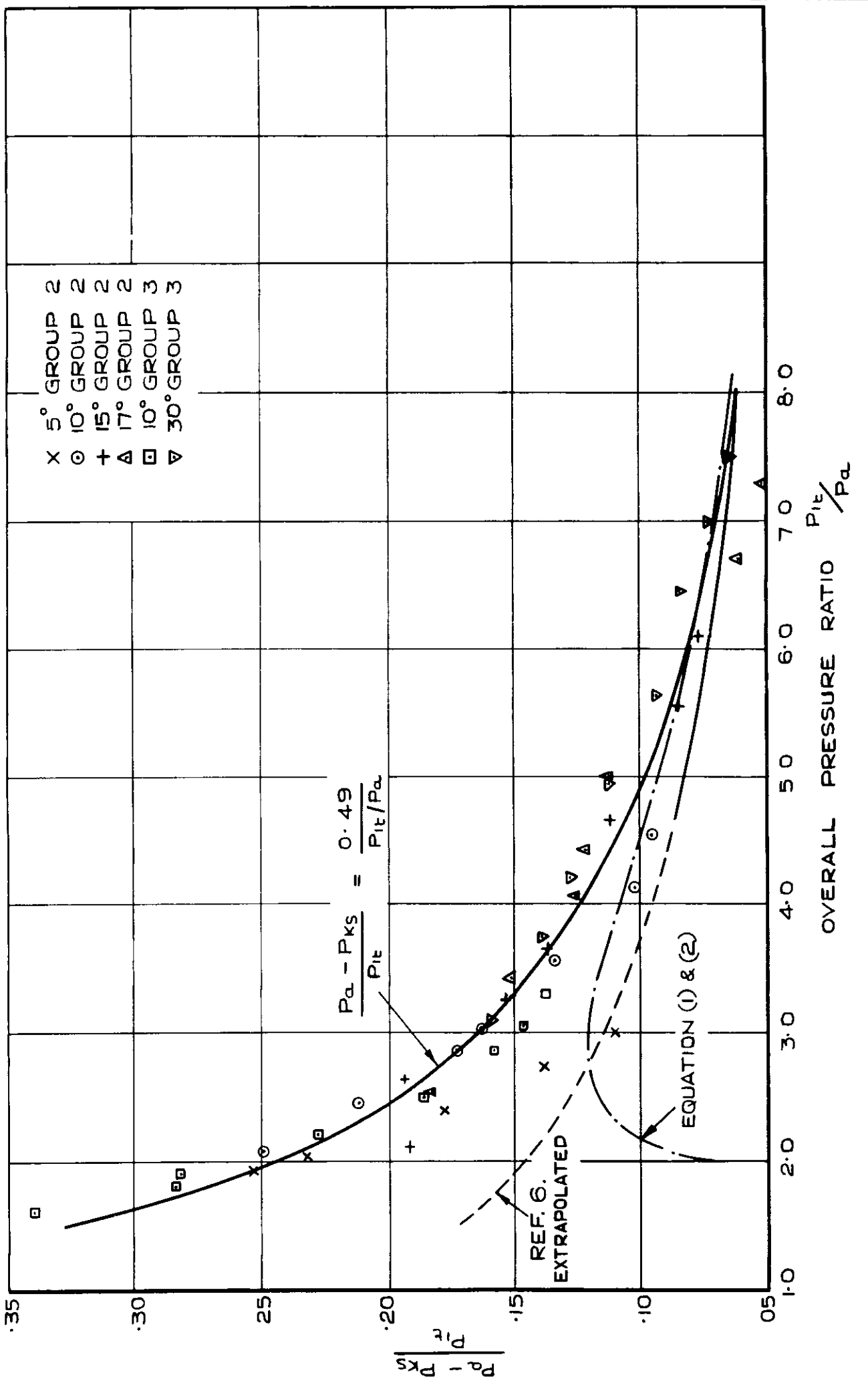

COMPARISON OF PRESSURE RISE PARAMETERS.

C.P. No. 327
(18,772)
A.R.C. Technical Report

Printed and published by
HER MAJESTY'S STATIONERY OFFICE

To be purchased from
York House, Kingsway, London W.C.2
423 Oxford Street, London W.1
13A Castle Street, Edinburgh 2
109 St Mary Street, Cardiff
39 King Street, Manchester 2
Tower Lane, Bristol 1
2 Edmund Street, Birmingham 3
80 Chichester Street, Belfast
or through any bookseller

Printed in Great Britain

S.O. Code No. 23-9010-27

C.P. No. 327